

OPEN ACCESS

## Structure of Correlations in Fe<sub>99</sub>Zr<sub>10</sub> Spin Glass

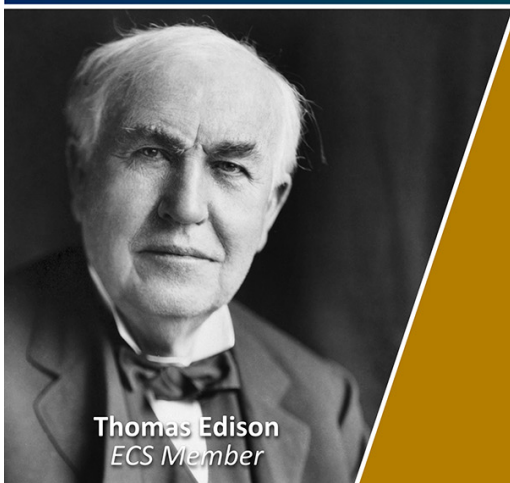
To cite this article: K Mergia and S Messoloras 2012 *J. Phys.: Conf. Ser.* **340** 012069

View the [article online](#) for updates and enhancements.

### You may also like

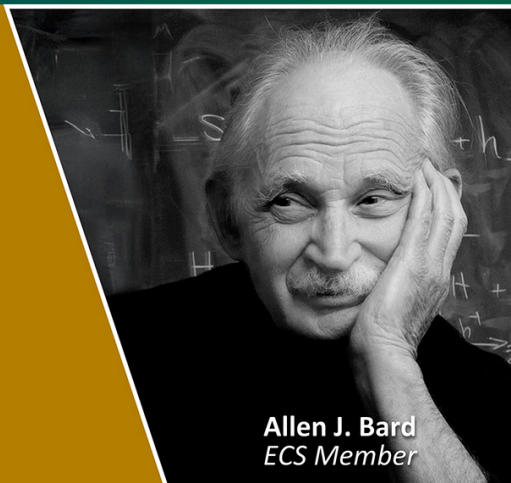
- [Strengthening mechanism and thermal deformation behavior of Al-12Si/Fe piston composite](#)  
Hao Yang, Yuan Wang, Xiuchang Wang et al.
- [Study on the strengthening mechanism of graphene and crystalline Cu<sub>3</sub>Fe on amorphous Fe<sub>3</sub>Cu](#)  
Yong-chao Liang, Shao-cong Zhou, Chao Yang et al.
- [Magnetic ordering of the martensite phase in Ni-Co-Mn-Sn-based ferromagnetic shape memory alloys](#)  
Sudip Kumar Sarkar, Sarita Ahlawat, S D Kaushik et al.

Join the Society  
Led by Scientists,  
for *Scientists Like You!*



The  
Electrochemical  
Society

Advancing solid state &  
electrochemical science & technology



## Structure of Correlations in Fe<sub>90</sub>Zr<sub>10</sub> Spin Glass

**K Mergia and S Messoloras**

Institute of Nuclear Technology and Radiation Protection, National Centre for Scientific Research "Demokritos", GR-15310 Aghia Paraskevi Athens, Greece

E-mail: kmergia@ipta.demokritos.gr

**Abstract.** There are various representations for the long time evolution and the dynamics of spin glasses, but a coherent, overall accepted real space description remains lacking. Small-Angle Neutron Scattering measurements reveal the long range spin-spin correlations from which the correlation length as a function of the temperature, time or magnetic field can be deduced. The scattering of the amorphous Fe<sub>90</sub>Zr<sub>10</sub> alloy during zero magnetic field cooling arises from long range correlations described by a Lorentzian function and scattering from spin clusters. From the temperature dependence of the correlation length two transitions are observed without, however, the correlation length to diverge. The application of magnetic field suppresses the transitions. The experimental findings are discussed in conjunction with different theoretical models.

### 1. Introduction

The study of amorphous FeZr alloys has attracted a lot of interest, mainly, because different magnetic behaviours can be realized by varying the iron content [1-10]. Three different types of magnetic behaviour have been observed in Fe<sub>100-x</sub>Zr<sub>x</sub> alloys, specifically i) ferromagnetic alloys for x=12 which are characterized by a Curie temperature  $T_c$ , ii) re-entrant spin glasses (RSG) for x=9-10 that are characterised by two transition temperatures,  $T_c$  which refers to the transition from the paramagnetic (PM) to the ferromagnetic (FM) state and  $T_f$  which refers to the transition from the FM state to the spin glass (SG) state and iii) spin glasses for x ≤ 8, in which one transition takes place from the PM to SG state at the temperature  $T_g$  [1-6]. The temperature  $T_c$  varies strongly with the Zr concentration and decreases as the Zr content increases [1, 7], whereas  $T_f$  varies in the opposite way and coincides with  $T_g$  for x=7 [1].

TEM and Lorentz microscopy studies on Fe<sub>90</sub>Zr<sub>10</sub> amorphous films showed the existence of magnetic domains with a configuration that remains the same upon cooling through the re-entrant spin-glass phase [8, 9]. Senousi et al [9] concluded that the main reason for the existence of the re-entrant behaviour is the anisotropy of the magnetic domains and that the long range ferromagnetic order is little perturbed by the spin-glass re-entrant transition.

The focus of the paper is a neutron scattering study of the magnetic correlations, the nature of the phase transitions and the response to applied magnetic field of the amorphous Fe<sub>90</sub>Zr<sub>10</sub>.

## 2. Small Angle Neutron Scattering from Spin Glasses

The scattering from a magnetic system, in the static approximation, is described by its spin-spin correlation function  $g(r)$  (isotropic system) which can be separated into two parts, the one describing the long range correlation  $g_{lr}(r)$  and the other the short range one  $g_{sr}(r)$ . The neutron scattering is then given by [11]

$$S(Q) = F\{g_{lr}(r)\} + F\{g_{sr}(r) - \langle g(r) \rangle\} \quad (1)$$

where  $F\{ \}$  denotes the sine Fourier transform i.e. for a system with spherical symmetry

$$F\{g(r)\} = \frac{1}{A} \int g(r) r^2 \frac{\sin Qr}{Qr} dr, \quad A = \int g(r) r^2 dr \quad (2)$$

$\langle g(r) \rangle$  is the averaging over the whole sample volume and  $|\mathbf{Q}| = 4\pi \sin \theta / \lambda$  ( $2\theta$  is the scattering angle and  $\lambda$  is the neutron wavelength). The first term in equation (1) gives the scattering at high  $Q$  values (Bragg scattering in a polycrystalline sample), whereas the second term corresponds to SANS scattering. As the scattering is conserved, loss of scattering from the SANS region implies that the short range order has been transformed to a long range one (within the term long range is included the scattering from constant magnetization). Notwithstanding that in the low  $Q$  region the length scale observed is of the order  $Qd \sim 2\pi$ , abrupt changes in the observed scattering indicate the transition to long order or absence of them indicate that the system has not undergone a long range order transitions (e.g. from paramagnetic to FM).

In a ferromagnetic system the neutron scattering in the static approximation for temperatures  $T > T_c$  is described by the a Lorentzian [6]

$$I(Q) = \frac{A\kappa^2}{\kappa^2 + Q^2} \quad (\text{Lor}) \quad (3)$$

where  $\kappa$  is the inverse spin correlation length,  $\xi$ , given by  $\xi = 1/\kappa$ . This form of scattering is derived from the spin correlation function of Ornstein-Zernicke type, i.e.

$$\langle \mathbf{S}_i(0) \circ \mathbf{S}_j(\mathbf{r}) \rangle_T \sim \frac{1}{r^{(d-1)/2}} \exp(-\kappa r) \quad (4)$$

for dimensionality  $d$  equal to 3.

In a system in which random fields exist the correlation function can be described by [13-14]

$$\langle \mathbf{S}_i(0) \circ \mathbf{S}_j(\mathbf{r}) \rangle_T \sim \frac{1}{r^{(d-3)/2}} \exp(-\kappa r) \quad (5)$$

This correlation function for  $d = 3$  gives the following form for the neutron scattering

$$I(Q) = \frac{B\kappa^4}{(\kappa^2 + Q^2)^2} \quad (\text{Lor}^2) \quad (6)$$

If  $d_l$  the dimensionality of the system below which the system cannot preserve long range order, then, for lower dimensionalities the neutron scattering is described by the sum of a Lor and a Lor<sup>2</sup> function. The correlation length,  $\xi$ , might be different for the Lor or Lor<sup>2</sup> functions [15]. The form of

the correlation function recently has attracted new attention [16]. Both  $Lor$  and  $Lor^2$  curves can be easily distinguished from the usual Guinier approximation at low  $Q$  values.

### 3. Experimental

Initially the polycrystalline alloy  $Fe_{90}Zr_{10}$  was fabricated from pure (99.99%) constituent metals by arc melting under argon atmosphere. Weight losses were small and less than 0.1%. Amorphous ribbons were produced by fast cooling of the melt alloy on a rotating wheel giving a cooling rate of  $10^6$  K/s and in an argon atmosphere. No weight loss was detected during the fabrication of the amorphous ribbons from the melt alloy. The thickness of the produced ribbons was around  $10\ \mu m$  and their width around 3 mm, exhibiting high elasticity consistent with their amorphous state. In addition XRD measurements showed no crystallinity. The SANS measurements were carried out at the LOQ instrument at ISIS neutron spallation source facility, in U.K. in the temperature range 10 to 300 K. The magnetic field was applied in the horizontal direction

In this work we shall discuss two types of experimental procedures, a) zero field cooling (ZFC) and b) field cooling (FC).

### 4. Results

#### 4.1 Zero field cooling

SANS measurements in zero magnetic field at low temperatures show the spontaneous changes of the magnetic state of the sample as structural changes can not be induced. However, the reversibility of the magnetic state prepared during a cooling process can not be taken for granted [17]. For example, the melting temperature of spin clusters produced at low temperatures will depend on the heating rate. Thermodynamic reversibility, even if it exists, will be observed for a process as slow as restricted by the dynamics of the system. It is, therefore, important to determine the reversibility of either a  $\Delta T$  change or of a full cycle. The holding time for a SANS measurement is about 30 min whereas 10 K temperature change has a duration of about 5 min. So reversibility or irreversibility is discussed in this time context.

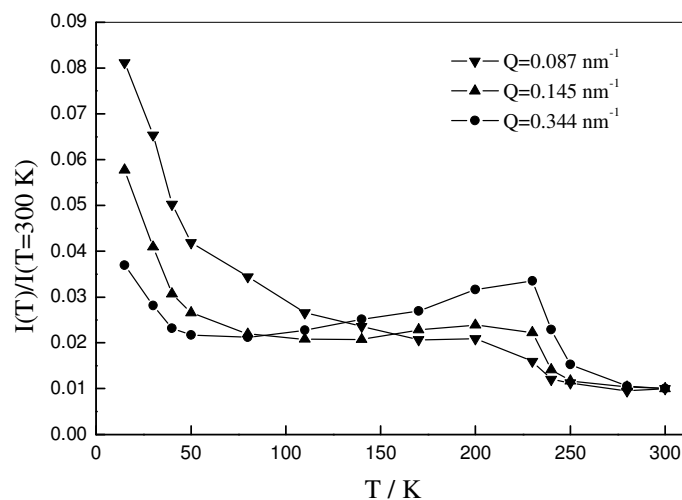


**Figure 1.** SANS for ZFC versus temperature for different values of  $Q$ .

The SANS increases during ZFC (from 300 down to 15 K) and it has been verified that the scattering is fully reversible, both step-wise or as a cycle, for ZF warming up. From 300 down to 250 K the scattering remains almost constant. The ratio of the scattering to that at  $T=300$  K versus

temperature and for three different  $Q$  values is presented in figure 1. As discussed above all changes in the SANS arise from changes in the spin-spin correlation function and not from any structural changes. Therefore, the increase in SANS at 230 K reflects that the uncorrelated spins of the paramagnetic state of room temperature develop correlations. Magnetization measurements show that there is a transition at  $T_c=240$  K which has been attributed to a PM to FM transition [18]. However, these correlations can not be of long range as the scattering at, for example,  $Q = 0.145 \text{ nm}^{-1}$  reflects structure in the range of 45 nm. Around 130 K a cross over for the different  $Q$  values is observed and as the temperature decreases the scattering increases with an apparent maximum at zero temperature. The faster increase of the smaller  $Q$  values shows that now spin correlated sizes larger than those of the transition at 230 K are being grown. The strong development of the second transition could be assigned at around 40 K whereas the transformation continues down to 15 K.

As discussed in section 2 the SANS data can be fitted by a Lor or Lor+Lor<sup>2</sup> functions (equations 3 and 6) as it has been for the amorphous Fe<sub>91</sub>Zr<sub>9</sub> alloy [19]. However, such functional forms do not fit the SANS curves in any temperature range. That Lor or Lor+Lor<sup>2</sup> functions do not fit the SANS data have been also been found in the SANS measurements in a series of FeZr alloys [20]. They have chosen to fit the SANS data using a Lor function plus a complicated form presenting spin clusters.

Also in our case, we find that the SANS curves show that two sources of scattering exist. The first can be represented by a Lor function, whereas the second has a  $Q^{-4}$  dependence which is the Porod approximation [21]. The presence of the Porod law implies that two magnetic phases exist which have different magnetizations (SANS arises from a different magnetic contrast) and that they are separated by sharp interfaces. This is in agreement with Lorentz microscopy studies on Fe<sub>90</sub>Zr<sub>10</sub> films which show that magnetic regions exist in all temperatures down to 6 K and that the structure of these regions does not change during the cooling below  $T_c$  [9]. All the SANS measurements have been fitted by the functional form

$$I(Q) = \frac{A\kappa^2}{\kappa^2 + Q^2} + \frac{C}{Q^4} = \frac{A\kappa^2}{\kappa^2 + Q^2} + \frac{\alpha S |(\mathbf{M}_p - \mathbf{M}_m) \times \mathbf{n}_Q|^2}{Q^4} \quad (7)$$

where  $S$  the total surface of the scattering particles,  $\mathbf{M}_p$  the mean magnetization of one particle,  $\mathbf{M}_m$  the mean magnetization of the matrix and  $\mathbf{n}_Q$  the unit vector along the direction of the scattering vector  $\mathbf{Q}$  and  $\alpha$  a constant that accounts for the correct units.

Figure 2 shows the scattered intensity as a function of  $Q$  at several temperatures during ZFC and the continuous lines are least square fits of equation 7 to the experimental data. From the least square fits the values for  $\xi$ ,  $A$ , and  $C$  have been determined and are depicted in figures 4 and 5 as a function of temperature.

The  $\xi$  value at room temperature (RT) is large (22.4 nm) and decreases as the temperature decreases to 250 K, followed by an increase as the temperature approaches  $T_c \approx 230$  K. Further it presents a slow decrease towards 60 K, whereas further decrease of the temperature results in its abrupt increase to around 10 nm. This behaviour of the correlation length is completely different to that observed in a Fe<sub>91</sub>Zr<sub>9</sub> alloy [19]. Also, later measurements on the same concentration alloy [20] show completely different behavior. Sample differences should be excluded as the same group carried out both measurements. However, it should be noted that between these two measurements different not overlapping  $Q$ -ranges and different fitting procedures were used. Our  $Q$ -range, due to the wide wavelength range available at the LOQ instrument, covers both  $Q$ -ranges used. Therefore, whether a function fits the data is more stringently tested and both long and short wavelength correlations are measured. It should also be added that it is not apparent if the Lor function fitted to the previous SANS

data corresponds to our equation 3 which is the Fourier transform of Ornstein-Zernicke correlation function i.e. our constant  $A$  is correlation length independent.

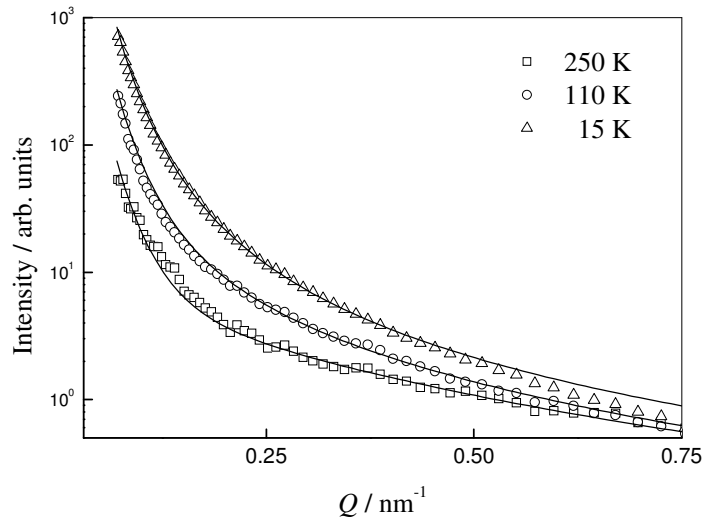


**Figure 2.** SANS versus  $Q$  at different temperatures during ZFC. The continuous lines are least square fits to the data according to equation (7).

This temperature variation of both correlation length,  $\xi$ , and constant,  $A$ , indicates the presence of the two transitions as described before. The constant  $C$  presents a continuous increase as the temperature decreases, which becomes abrupt below 50 K. This variation of  $C$  can be explained either with the size increase of the spin clusters or with the increase of the magnetic contrast between the clusters and the matrix (equation 7). This will be discussed later on, after the description of the sample behaviour under the other processes.

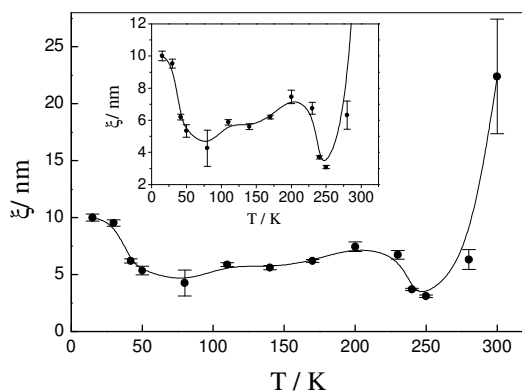


**Figure 3.** Spin correlation length as a function of temperature during ZFC. The inset is a zoom. The continuous lines are guide to the eye.

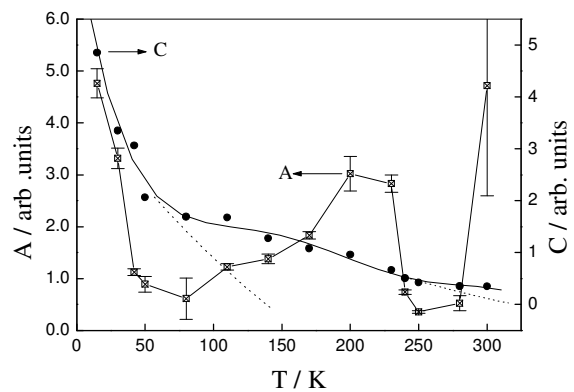


**Figure 4.** The constants  $A$  and  $C$  of equation 10 as a function of temperature during ZFC. The continuous lines are guide to the eye.

#### 4.2 Field cooling

The application of a magnetic field at 300 K reduces the scattered intensity. This reduction is initially proportional to the magnetic field magnitude and for fields larger than 0.5 T no further change is observed. The scattering at RT with field off is described by the equation 7. With the application of a magnetic field ( $>0.16$  T) the second term is not required to describe the scattering and  $I(Q)$  presents a  $1/Q^2$  behaviour. This is proved by the linear dependence of  $\ln(I(Q))$  versus  $\ln(Q)$  having a slope equal to 2 for all field values larger than 0.16 T (figure 5).

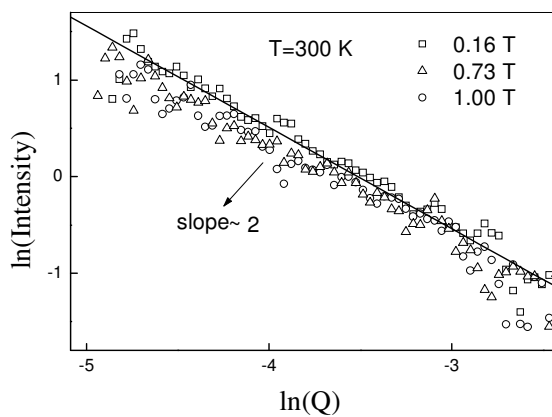


**Figure 5.** Variation of the logarithm of the scattered intensity versus the logarithm of  $Q$  at RT for various field values.

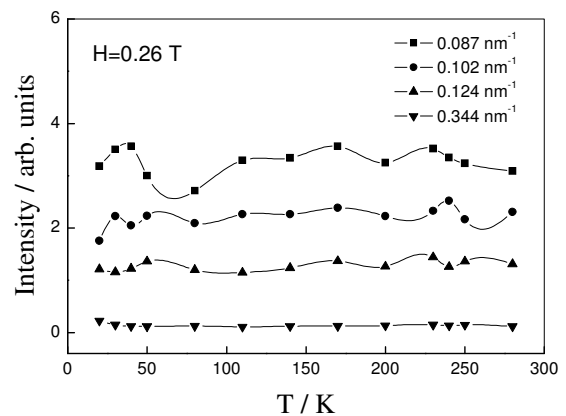


**Figure 6.** Variation of the scattered intensity versus temperature for various  $Q$  values, during FC in a field of 0.26 T.

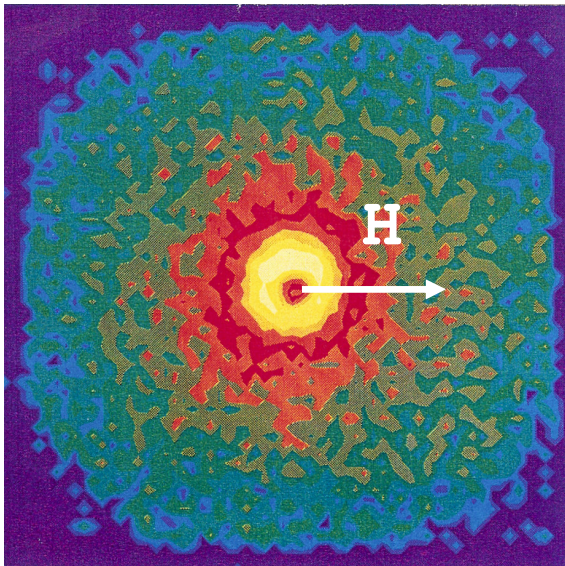


**Figure 7.** Constant scattered intensity contour from the area detector for  $H=0.26$  T at 30 K during FC.

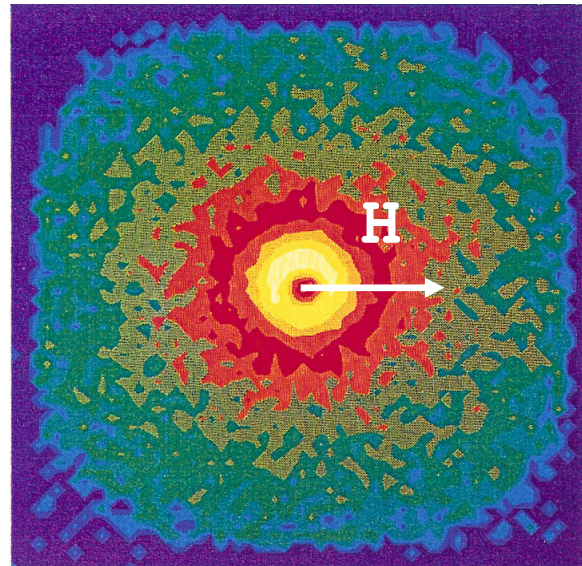


**Figure 8.** Constant scattered intensity contour from the area detector at 20 K after removal of the field.

During FC from 280 to 20 K in a magnetic field of 0.26 T no variation in the scattered intensity versus temperature is observed, as it is depicted in figure 6, and none of the phase transitions observed in the ZFC occurs. The scattering in this temperature range can be described by the equation

$$I(Q) = \frac{B}{Q^2} + \frac{C}{Q^4} \quad (8)$$

During FC the value for constant  $C$  is at least one order of magnitude lower than that determined during ZFC.

In all temperatures during FC the scattered intensity on the 2D detector presents elliptical distortion with the maximum scattering occurring perpendicular to the applied field direction (figure 7). Such prolate distortion is expected from an ensemble of ferromagnetic clusters. After the removal of the field at 20 K the scattering becomes oblate (figure 8).

## 5. Discussion and Conclusions

The purpose of this work is to understand the nature of the two transitions of this amorphous alloy at the so called  $T_c$  and  $T_f$  temperatures. Initially, we have to understand the magnetic state of the sample at room temperature. The SANS from the amorphous Fe<sub>90</sub>Zr<sub>10</sub> alloy at RT is described by the equation 7 which involves two terms. This fact indicates that there are two scattering sources. One comes from a spin correlation function (equation 4,  $d=3$ ) that gives rise to the Lor type scattering and the other comes from a magnetization contrast that gives rise to a Porod like scattering. The presence of Porod scattering suggests the existence of magnetic clusters with different magnetization than that of the matrix. It should also be noted that the Porod law dependence implies sharp interfaces between the two magnetic phases. So, two magnetic phases co-exist at room temperature. The local extent of either phase has to be above 120 nm in diameter, otherwise the Porod law would not have been observed (the Porod law is an asymptotic form of scattering which applies for  $QR > 4$ ). The word phase here has the meaning of a magnetic moment spatial configuration. From the second term in equation (7) it is apparent that configurationally different phases could arise from magnetic moment differences either in orientation or in magnitude. The first possibility would reflect magnetic domain formation whereas the second should be the result of structural differences either in the Fe concentration or in sample crystallinity. However, it should be remembered that these regions are large and separated with sharp interfaces. The Lor term indicates that within one phase or both or at the interface of these two phases spin-spin correlations of about 24 nm exist.

In the previous paragraph it has been established that at RT two regions with different magnetizations co-exist and these two regions are separated with sharp interfaces. For the description of the system the two phase magnetic model is most suitable [23]. Within this picture the spin misalignment scattering [24] is thought insignificant and it is ignored. This conclusion is based on that the explicit angular dependence of the spin misalignment contribution is not observed before or after the application of the magnetic field (figure 7). Therefore the model we are thinking is that of a magnetic inhomogeneity embedded in a matrix. We shall call the magnetic inhomogeneity spin cluster implying simply that its spins behave the same way. The magnetic moments of spin clusters and matrix at RT are different both in magnitude and possibly in direction and one of them might be zero (paramagnetic). Also, if they undergo a phase transition it would be expected to occur at different temperatures. In order to understand the magnetism of these two regions, we shall next discuss the dependence of the SANS on magnetic field at RT and the temperature change of the constant  $C$  (figure 4 and equation (7)).

The SANS at 300 K in a magnetic field above 0.6 T shows a  $1/Q^2$  dependence. For lower fields the SANS is described by equation (7). This implies that the application of the magnetic field has two effects, a) the correlation length arising for the Lor function becomes very large and b) the magnetic contrast difference between the two phases becomes zero (Porod scattering, second term of equation

7). The Porod scattering without magnetic field is isotropic, with the application of a small field it becomes anisotropic and as the field increases, it decreases to become zero for fields equal and above 0.6 T. The anisotropic SANS implies magnetic inhomogeneities and that the magnetic moment of the inhomogeneities (or of the surrounding matrix) has a definite angle with the magnetic field. Since the magnetic contrast decreases as the field increases, we have to assume that a) the spins in the matrix are aligned with the application of a small magnetic field and b) as the field increases the magnetic moments of the cluster rotate to be finally aligned with the field. As, finally, the magnetic contrast becomes zero we have to accept that the magnitude of the magnetic moments in both the spin cluster and the matrix are almost equal. The fact that a small magnetic field destroys both the short (Lor function, equation (7)) and long wavelength (Porod scattering) correlations indicates that both the spin clusters and the matrix are very close to a ferromagnetic transition. The FM transition here has the meaning that the spins on average are aligned to the applied magnetic field. Therefore, from the application of the magnetic field at RT the picture which emerges is as follows: a) a small magnetic field aligns the spins of the matrix but its average magnetic moment is different than that of the spin clusters (this explains that the isotropic without magnetic field SANS becomes anisotropic after the application of a small magnetic field), b) as the field increases the mean magnetic moment of the spin clusters increases as it is demonstrated by the decrease of the constant  $C$  and c) at field of 0.6 T both the magnetic moments of the spin clusters and the matrix are equal giving  $C = 0$ . In this picture it has been implied that as the magnetic field increases the size of the spin clusters remains constant but their average magnetic moment increases. However, another possibility consistent with the experimental results exists. The spins at the surface of the cluster are partially influenced by the molecular field arising from the magnetization of the matrix. As the matrix spins are aligned in the applied magnetic field their magnetization increases. Now the spins on the cluster experience a stronger molecular field and the external field. The combination of these two fields becomes strong enough to align to the external magnetic field a shell of the spins of the cluster, thus reducing its size. In this picture the reduction of the constant  $C$  is attributed to the reduction of the size of the spin cluster and not predominantly to the alignment of its magnetic moments to the external magnetic field. This second interpretation of the experimental results is more appealing as it includes a plausible physical mechanism for the homogenization of the two magnetic regions.

During ZFC a “cusp” is observed at around 230 K (figure 1) the presence of which indicates a phase transition in agreement with ac susceptibility measurements on the same sample. Furthermore, at the same temperature a maximum in the values of  $\xi$  and  $A$  is observed, whereas this does not apply for the constant  $C$  (figures 3 and 4). In the previous paragraphs it has been established that there are two different magnetization regions which are described with the constant  $C$  (see equation (7)). In figure 4 the temperature change of the constant  $C$  can be interpreted as the superposition of two curves one which would indicate a phase transition above 300 K and the other at around 150 K (see extrapolated lines in figure 4). Keeping in line with the discussion of the previous paragraph in which the response of the system to the application of a magnetic field was discussed, the high temperature transition is attributed to the matrix whereas the lower temperature transition to the spin clusters.

Summarizing the above we may conclude that there is strong experimental evidence for the correctness of the model for re-entrant spin glasses that visualize such systems, in the ferromagnetic state, to be composed of an infinite three-dimensional (3D) FM cluster (matrix) and finite spin clusters [1, 25-27]. However, if for  $T_c$  we take the temperature of 240 K we do not observe a long range ferromagnetic order (figure 4, constant  $C$ ) as magnetization measurements have been interpreted [28] but the onset of a FM type transition of the matrix. The SANS results demonstrate that even small magnetic fields destroy the differentiation between matrix and clusters (figure 5), thus measurements even in a small magnetic field do not reveal the ground state of the system. SANS corresponds to the ground state of the system unperturbed by the application of a magnetic field thus, these type of measurements are invaluable in elucidating the re-entrant behaviour [29].

Having outlined above the physical processes reflected in the second term of equation 7, we now focus our discussion to the results arising from the Lor part of equation (7) which corresponds to the correlation function given by equation 4. The physical parameters derived from the SANS data fitting are the correlation length,  $\xi$ , and the constant,  $A$ , which is proportional to the strength of the magnetization i.e.  $A = \langle \mathbf{S}^2 \rangle_T$ . Both constants show a transition at 230 and 40 K (see figures 3 and 4). In the magnetization measurements a bifurcation of the heating and cooling curves is observed at a temperature so called freezing temperature  $T_f$  [30]. The extrapolated freezing temperature to zero field derived from magnetization measurements is 40 K [31] which corresponds to the fast increase of the SANS observed in figure 1. The lower temperature transition has been attributed to a transition from the ferromagnetic state to a micromagnetic (cluster spin-glass state) state. It should be noted that the magnetization fails to saturate at 4.2 K and in fields of 15 T [32]. The continuous increase of SANS (figure 1) as the temperature decreases is consistent with the lack of magnetic moment saturation. These two magnetic phase transitions are also observed in resistivity measurements [33]. Initially the room temperature specific resistivity decreases as the temperature decreases which is expected if the main contribution arises from electron-phonon scattering. At around 240K there is a plateau and below this temperature an almost linear increase in the specific resistivity is observed which apparently could be attributed to an increase of the electron-spin scattering. Further, at around 30 K an abrupt change in the slope is observed. The magnetoresistance at a magnetic field of 8 T is positive at all temperatures and shows a maximum at around  $T_c$  [34]. From both high field magnetization and Mössbauer measurements at 4.2 K the magnetic moment is  $1.75 \mu_B/\text{Fe atom}$  [35]. We conclude this paragraph by restating that the two magnetic transitions demonstrated in figures 1, 2 and 3 have been observed at around the same temperatures by different experimental techniques.

The two transitions of the correlation length and constant  $A$  at 230 and 40 K are obviously connected with the transition of the matrix (240 K) and the spin cluster (40 K). That the phase transitions denoted by the parameters of the scattering described by the Lor function (equation 7) are connected with the phase transition of the matrix and the spin clusters points out that this scattering most probably arises from the interface of the two regions. It is, thus, proposed that at the spin cluster-matrix interface the competing interactions give rise to Ornstein-Zernicke type spin correlations i.e. the interface is always just before a FM transition. This proposition is corroborated with the fact the application of a magnetic field (ZFC) suppresses both transitions at 230 and 40 K.

Concluding we may suggest that this work offers two contributions in the understanding of the re-entrant spin glasses. It establishes that there are two magnetically different regions which have different transition temperature to FM order. Small magnetic fields can switch both these regions to a common FM state. Further the competing interaction at the interface of these regions results to short wavelength (10 nm) spin correlations which also follow the phase transitions of the two regions. A small magnetic field suppresses these transitions as it is stronger than the internal fields generated at the interface of the two magnetic regions. The findings of this work are in broad agreement with a recent theoretical description of the re-entrant spin glass system [36].

### Acknowledgments

We would like to thank the British Council and the Greek General Secretariat of Research and Technology for financial support. The experiments at the ISIS Pulsed Neutron and Muon Source were supported by a beamtime allocation from the Science and Technology Facilities Council. The contribution of Dr. S. King during the experiments is appreciated.

### References

- [1] Kiss L F, T. Kemény T, Vincze I and Gránásy L 1994 *J. Magn. Magn. Mater.* **135** 161
- [2] Hiroyoshi H and Fukamichi K 1982 *Physics Letters* **85A** 242
- [3] Ryan D H and Coey J M D 1987 *Phys. Rev. B* **35** 242

- [4] Kaul S N 1983 *Phys. Rev. B* **27** 6923
- [5] Read D A, Moyo T and Hallam G C 1984 *J. Magn. Magn. Mater.* **44** 279
- [6] Beck W and Kronmueller H 1985 *Phys. Stat.. Solidi (b)* **132** 449
- [7] Ryan D H, Coey J M D, Batalla E, Altounian Z and Strom-Olsen J O 1987 *Phys. Rev. B* **35** 8630
- [8] Wronski Z, Janicki A J and Matyja H 1983 *J. Mater. Sci. Lett.* **2** 5
- [9] Senoussi S, Hadjoudj S, Jouret P, Bilotte J and Fourmeaux R 1988 *J. Appl. Phys.* **63** 4086
- [10] Mergia K, Messoloras S, Nicolaidis G, Niarchos D and Stewart R J 1996 *J. Appl. Phys.* **76** 6380
- [11] Mergia K and Messoloras S 2008 *J. Phys.: Condens. Matter* **20** 104219
- [12] Marschall W and Lovesey S W 1971 *Theory of Thermal Neutron Scattering*
- [13] Aharony A, Imry Y and Ma S -K 1976 *Phys. Rev. Lett.* **37** 1367
- [14] Grinstein G 1976 *Phys. Rev. Lett.* **37** 944
- [15] Aharony A and Pytte E 1983 *Phys. Rev. B* **27** 5872
- [16] Dominicis C de, Giardina I, Marinari E, Martin O C and Zuliani F 2005 *Phys. Rev. B* **72** 014443
- [17] Cugliandolo L F and Kurchan J 1999 *Phys. Rev. B* **60** 922
- [18] Buschow K H J and Smit P H 1981 *J. Magn. Magn. Mater.* **23** 85
- [19] Rhyne J J and Fish G E 1985 *J. Appl. Phys.* **57** 3407
- [20] Rhyne J J, Erwin R W, Fernandez- Baca J A and Fish G E 1988 *J. Appl. Phys.* **63** 4080
- [21] Porod G 1951 *Kolloid-Z* **124** 83; Porod G 1952a *Kolloid-Z* **125** 51; Porod G 1952b *Kolloid-Z* **125** 108
- [22] Burke S K, Cywinski R and Rainford B D 1978 *J. Appl.. Cryst..* **11** 644
- [23] Löffler J F, Braun H B, Wagner W, Kostorz G and Wiedenman A 2005 *Phys. Rev. B* **71**, 134410
- [24] Michels A and Weissmüller J 2008 *Rep. Prog. Phys.* **71** 066501
- [25] Coles B R, Sarkissian B V B and Taylor R H 1978 *Phil. Mag. B* **37** 489
- [26] Kaul S N 1980 *Solid State Commun.* **36** 279
- [27] Kaul S N 1985 *J. Magn. Magn. Mater.* **53** 5
- [28] Kaul S N 1988 *J. Phys. F: Met. Phys.* **18** 2089
- [29] Srinath S and Kaul S N 2000 *Europhys. Lett.*, 51 441
- [30] Kaul S N and Srinath S 1998 *J. Phys.: Condens. Matter* **10** 11067
- [31] Kaul S N 1983 *Phys. Rev. B* **27** 6923
- [32] Krishnan R, Rao K V and Liebermann H H 1984 *J. Appl. Phys.* **55** 1823
- [33] Obi Y, Wang L C, Motsay R and Onn D G 1982 *J. Appl. Phys.* **53** 2304
- [34] Dahlberg D, Rao K V and Fukamichi K 1984 *J. Appl. Phys.* **55** 1942
- [35] Unruh K M and Chien C L 1983 *Phys. Rev. B* **30** 4968
- [36] Niidera S and Matsubara F 2007 *Phys. Rev. B* **75** 14413